Research Article

MOLECULAR PAIN

Molecular Pain
Volume 12: 1–11

DOI: 10.1177/1744806916684515
journals.sagepub.com/home/mpx

SAGE

Characterization of the anterior cingulate cortex in adult tree shrew

Jing-Shan Lu[1], Fang Yue[1], Xiaoqing Liu[1], Tao Chen[1,2] and Min Zhuo[1,3]

Abstract

The anterior cingulate cortex (ACC) is a key brain region for the perception of pain and emotion. Cellular and molecular mechanisms of the ACC are usually investigated in rodents such as mice and rats. Studies of synaptic mechanisms in primates are limited. To facilitate the translation of basic results from rodents to humans, it is critical to use a primate-like animal model for the investigation of the ACC. The tree shrew presents a great opportunity for this as they have similar genome sequences to primates and are considered to have many similarities to primates. In the present study, by combining anatomy, immunostaining and micro-optical sectioning tomography methods, we examined the morphological properties of the ACC in the tree shrew and compared them with the mouse and rat. We found that the ACC in the tree shrew is significantly larger than those found in the mouse and rat. The sizes of cell bodies of ACC pyramidal cells in tree shrew are also larger than that found in the mouse or rat. Furthermore, there are significantly more apical/basal dendritic branches and apical dendritic spines of ACC pyramidal neurons in tree shrew. These results demonstrate that pyramidal cells of the ACC in tree shrews are more advanced than those found in rodents (mice and rats), indicating that the tree shrew can be used as a useful animal model for studying the cellular mechanism for ACC-related physiological and pathological changes in humans.

Keywords

Tree shrew, anterior cingulated cortex, mouse, rat, pyramidal cell, pain, pleasure

Date received: 6 September 2016; revised: 16 November 2016; accepted: 22 November 2016

Introduction

Acute pain is considered as a signal which allows animals and humans to learn about potentially dangerous threats, which also often called physiological pain. Chronic pain, or pathological pain by contrast, is often caused by injuries or specific disease conditions, and it causes unpleasantness, discomfort, sadness, hopelessness, anxiety and depression over a longer period of time than acute pain. Among the cortical areas, the anterior cingulate cortex (ACC) and insular cortex are the two major areas which play important roles in coding functions for both acute and chronic pain.[1–3] By contrast, pleasure or happiness is the state of mind that animals and human pursue. It is often not long-lasting, unlike chronic pain. Human and animal studies suggest that neurons in the ACC may also contribute to the coding of pleasure.[4] Similar to reports from human studies, neurons in the ACC do respond to noxious stimuli and are activated by pleasure-like sex attraction.[4] Synaptic transmission and plasticity are found to play critical roles in chronic pain.[1,4,5] Rodents such as mice and rats are common animal models for studying the cellular and synaptic functions of the ACC.[1,2] Less synaptic information is available using primate models. Most of the previous studies in monkeys focused on

[1]Center for Neuron and Disease, Frontier Institute of Science and Technology, Xi'an Jiaotong University, Xi'an, China
[2]Department of Anatomy, Histology and Embryology and K.K. Leung Brain Research Center, the Fourth Military Medical University, Xi'an, China
[3]Department of Physiology, Faculty of Medicine, University of Toronto, Toronto, Ontario, Canada

Corresponding authors:
Tao Chen, Center for Neuron and Disease, Frontier Institute of Science and Technology, Xi'an Jiaotong University, Xi'an 710049, China.
Email: chtkkl@fmmu.edu.cn
Min Zhuo, Center for Neuron and Disease, Frontier Institute of Science and Technology, Xi'an Jiaotong University, Xi'an 710049, China.
Email: minzhuo10@gmail.com

the anatomy and electrophysiological properties of the ACC neurons in vivo. In vitro brain slice studies from primates are usually considered to be too costly and limited by strict regulations. Despite much similarity at the synaptic level between rodents and primates, there are several obvious differences. The life span of rodents are significantly shorter than that of primates, and some of the typical human aging brain markers such as amyloid β (Aβ) cannot be found in rodents brains.[6] Second, cortical pyramidal neurons in primates are highly developed, with more complex branches and spinal structures.[7,8] There is clearly a need for further investigation of the ACC in primates or primate-like animals to facilitate the translation of findings from rodents to humans, especially for understanding the molecular mechanisms of emotion and brain disease.

The tree shrew is a small squirrel-like mammal with a well-developed central nervous system. Due to its small body size, the low cost of breeding and short reproductive cycle, the tree shrew has been used as primate-like animal model for studying vision, learning and emotion.[9–14] Several observations support the claim that the tree shrew may present a useful primate model for the study of ACC functions. First, recent genetic studies indicate that the tree shrew is more similar to primates as compared with rodents.[15–17] Second, unlike rodents, the lifespan of tree shrew is three to four times longer (about 10 years).[18] Third, somatosensory and visual cortical regions in the tree shrew are highly developed and resemble those of primates.[7,19,20] Perhaps most interestingly, Aβ accumulation has been reported in the aged tree shrew.[6] This is similar to humans but not found in rodents. Therefore, we believe that the tree shrew can be used as a useful animal model for the investigation of physiological and pathological process of brain function in humans. In the present study, we investigated the morphological properties of the ACC in tree shrews and compared those with those of mice and rats. Our results indicate that the ACC in tree shrew is significantly better developed than in mice and rats. The pyramidal cells in the tree shrew also contain more densely distributed dendritic branches and spines suggesting that cortical neurons in tree shrews may be more widely and closely connected and have the ability to deal with more complicated information. Thus, as a unique experimental animal, the tree shrew has more powerful potential advantages for neurobiological research than the present widely used rodents.

Materials and methods

Animals

Adult male tree shrews (6–8 months) were purchased from Kunming Institute of Zoology in China. C57BL/6 mouse (6–8 weeks), Sprague-Dawley rat (8–10 weeks) and tree shrew were housed under a 12-h light and dark cycle with food and water provided ad libitum. All procedures and handling of animals were performed with permission according to the guidelines of Xi'an Jiaotong University.

Volume calculation of ACC

The animals were deeply anesthetized with Nembutal (30 mg/kg i.p.) and intracardially perfused with 20–35 ml saline followed by 100–500 ml of cold 0.1 M phosphate buffer (PB) containing 2% paraformaldehyde (Sigma-Aldrich, St. Louis, MO) for mouse, rat and tree shrew. The whole brain was taken out and weighed, and placed in 30% sucrose in 0.1 M PB. Then the brain containing ACC were serially cut into 100-μm serial coronal sections on a freezing microtome (Kryostat 1720; Leitz, Mannheim, Germany). One of two adjacent sections were collected and mounted on glass slides for imaging under bright field microscopy. The volume of ACC was calculated as a sectorial cylinder, according to the equation: (V, volume; L, sagittal length; S1, S2, rostral and caudal areas of ACC).

Nissl staining

The mouse, rat and tree shrew brains containing ACC were cut into serial coronal sections (20 μm) for Nissl staining. The sections were then mounted onto gelatin-coated glass slides and differentiated in 70% ethanol at 37°C overnight and stained in 0.1% cresyl violet solution for 20 min. After de-colorization in graded ethanol, the sections were dehydrated in ethanol, cleared in xylene and mounted with neutral resin.

Immunohistochemistry

The mouse, rat and tree shrew brains containing ACC were cut into serial coronal sections (20 μm). Then the sections were incubated with mouse anti-NeuN antibody (1:3000; Millipore Corporation, USA) in PBS containing 5% normal donkey serum, 0.3%Triton X-100, 0.03% NaN_3 and 0.25% carrageenan overnight at 4°C. The sections were then incubated with biotinylated donkey anti-mouse IgG (1:500, AP192B Millipore Corporation, USA) overnight at 4°C and fluorescein avidin D antibody (1:1000) for 2 h. Sections were then rinsed in PBS, mounted onto glass slides, air-dried, cover-slipped with a mixture of 50% (v/v) glycerin and 2.5% (w/v) triethylene diamine in 0.01 M PBS. The NeuN-positive neurons were visualized under confocal microscope (FV-1000; Olympus, Tokyo, Japan) under appropriate filter for fluorescein (excitation 495 nm; emission 519 nm).

Golgi staining

Animals were deeply anaesthetized and intracardially perfused with 20–35 ml saline. After that, the brain was immediately taken out and a coronal tissue block (1 cm × 1 cm × 0.5 cm) containing ACC was dissected. Each tissue block was stained by using Golgi-cox solution. Tissue blocks were placed in an ultraclean staining jar with Golgi-cox dye containing 1% potassium dichromate, 1% mercuric chloride and 0.8% potassium chromate. The jar was kept in the dark for 6 d while gently shaken. Tissue blocks were then affixed to a sectioning block and cut into 120 μm sections on a vibrating microtome (Leica VT1200 S, Leica, Germany). The sections were then mounted onto slides, air-dried, dehydrated in a series of graded alcohol, cleared in xylene and coverslipped. The neurons in the ACC area were photographed by a light microscope, and the number of neuron and spine density were calculated and summarized to the graph.

Micro-optical sectioning tomography analysis

Animals were anaesthetized and perfused with 0.1 M PBS solution (pH 7.4). The whole animal brains were taken out and placed in a brown vial with Golgi-cox dye for 10 days. Then the brains were cut (thick of 3.5 cm × 3.5 cm) and placed in 1% lithium hydroxide 24 h with shaking for melanism. After rinsing in distilled water for 24 h, the brain blocks were dehydrated in a series of graded ethanol: 50%, 70%, 85%, 95%, 100% ethanol/acetone (1:1) and then incubated in 100% acetone overnight. For osmosis, the brain blocks were kept in brown vial with freshly prepared spur resin series: 50%, 75%, 100%; 8 h each at room temperature. Brains were embedded in the silastic mold containing the spurr resin at 60°C for 36 h.

Animal samples were imaged automatically by Biomapping 1000 which is commercialized from the micro-optical sectioning tomography (MOST) technology.[21] About 3000 coronal slices (at 1 μm in thickness) were produced from original images of three animal samples individually by a series preprocessing steps, which include the cut of redundant image, alignment between neighboring image strips and the illumination calibration of whole slice. A series of projection images were generated from three preprocessed coronal images by minimum intensity projection of every 50 coronal slices or 100 slices. One can confirm the coronal range of ACC by browsing continuous projection images. Then three-dimensional data block including ACC can be extracted from continuous preprocessed coronal images by customized Matlab programs. Twenty pyramidal neurons of layer V were selected randomly from three data block individually for tracing and quantitative analysis. Then interactive neuron tracing was performed using the Filament Editor in Amira software. The classic Sholl analysis was chosen for the quantitative analysis of neural density, and the famous open source Trees Toolbox[22] was used to implement Sholl analysis. Some modification was performed on original Trees Toolbox for the quantitative analysis of basal dendrite and apical dendrite individually.

Statistics

All data were presented as the mean ± SEM and no data were excluded. Unpaired *t*-test or one-way ANOVA (Dunnett *t*-test was used for post hoc comparison) was used to make statistical comparisons among mouse, rat and tree shrew. The examples shown in all figures were representative and were reproducible at least three times for each set of experiments. In all cases, a probability value of $p < 0.05$ was considered statistically significant.

Results

General observation of tree shrew brain

The tree shrew looks similar to a squirrel and its size is a bit smaller than an average adult rat (Figure 1(a)). They reach maturity at six months and the lifespan is about 9 to 12 years.[17] We used six- to eight-month-old tree shrews in the present study. The average body weight of tree shrew was 136.8 ± 1.8 g (n = 8), which is much larger than mature mouse (24.4 ± 0.9 g, 8 weeks, n = 9) but smaller than rat (206.6 ± 13.7 g, 6 weeks, n = 9). We next fixed the brains of the three types of animals and examined their size and shape (Figure 1(b)). The mean brain weight of tree shrew was 3.14 ± 0.17 g (n = 8), 7.1 times heavier than mouse brain (0.44 ± 0.03 g, n = 9) and 1.8 times heavier than rat brain (1.72 ± 0.10 g, n = 9), respectively (Figure 1(c)). We then calculated the brain to body weight ratio and found that, in comparison with mouse (1.9 ± 0.2%) and rat (0.8 ± 0.1%), the brain/body ratio in tree shrew (2.6 ± 0.1%) is higher ($p < 0.05$).

The range and volume of ACC in tree shrew

To clearly identify the frame of the ACC, 100-μm coronal sections in the forebrain from the rostral beginning of orbital cortex to the caudal ending of diencephalon was serially cut and numbered. According to the criteria of mouse and rat Brain Atlas for the range of the ACC, we identified the range of the ACC in tree shrew was followed the caudal edge of prefrontal cortex and ended in the level with the appearance of hippocampus (from No. 52 to No. 94 sections in Figure 2, n = 3). On coronal section, ACC formed a sectorial area, with two straight side edges adjacent to motor cortex and one curved bottom above corpus

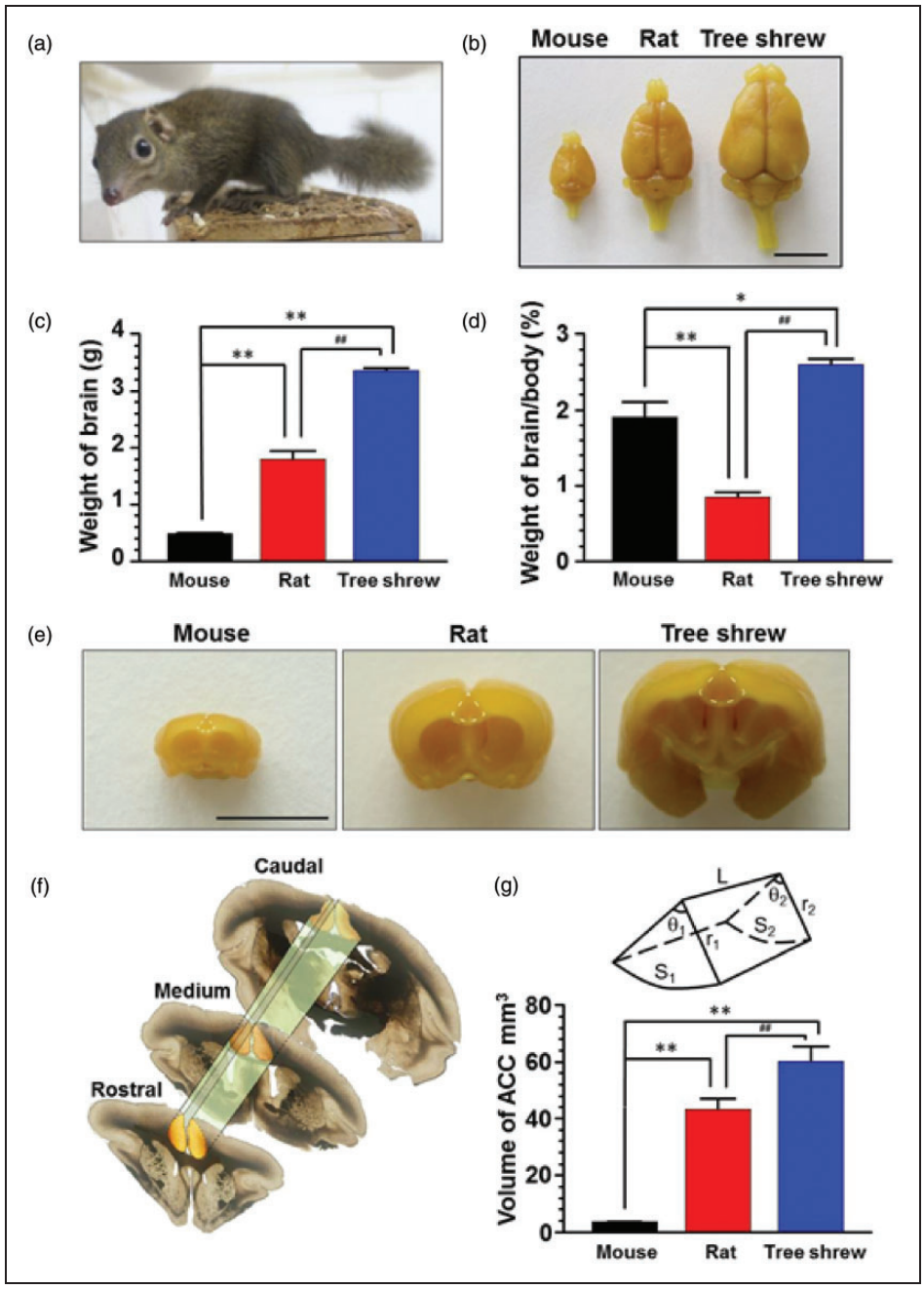

Figure 1. The anatomical property of the brain in tree shrew. (a) A photo of tree shrew in daily life. (b) Fixed whole brain of mouse, rat and tree shrew. Scale bar, 1 cm. The weight (c) and proportion of brain (d) in tree shrew were much larger than that of mouse and rat ($n = 9, 9, 8$ for mouse, rat and tree shrew), $^{*}p < 0.05$; $^{**}p < 0.01$ in comparison with mouse, $^{\#\#}p < 0.01$ in comparison with rat. (e) Representative coronal sections of forebrains in mouse, rat and tree shrew. The dash lines delineate ACC regions. Scale bar, 1 cm. (f) Sample sections showing the rostral, medium and caudal part of ACC in tree shrew. The integrated ACC was framed by dash lines. (g) The diagram showing the cylinder shape of ACC with sectorial section. S1, rostral areas of ACC; r1, radius of rostral ACC; θ1, degree of rostral ACC; S2, caudal areas of ACC; r2, radius of caudal ACC; θ2, degree of caudal ACC. Statistic results showing the volume of ACC was progressively increased in mouse, rat and tree shrew ($n = 3$ in each group), $^{**}p < 0.01$ in comparison with mouse, $^{\#\#}p < 0.01$ in comparison with rat.

callosum (Figures 1(e) and 2). Although there was no obvious morphological differences, corpus callosum in the tree shrew stretched deeper into the ACC than in that of mouse and rat (Figure 2). Meanwhile, the long and horizontal axis of ACC in tree shrew is much longer (long axis: mouse 2.03 ± 0.09 mm, rat 3.63 ± 0.12 mm, tree shrew 4.87 ± 0.28 mm; horizontal axis: mouse 1.64 ± 0.02 mm, rat 3.99 ± 0.11 mm, tree shrew

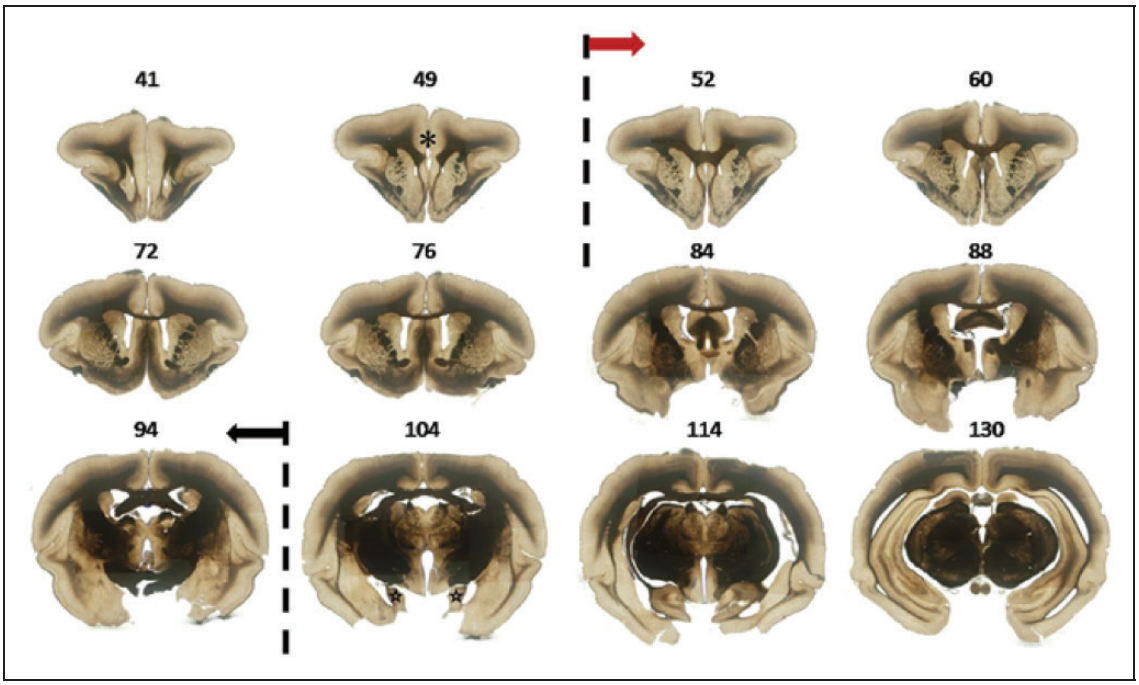

Figure 2. The representative serial sections showing the range of ACC in tree shrew. Sample sections from a stack of 100-μm serial coronal sections. In No. 49 section, prefrontal cortex was indicated by asterisk. Sections from No. 52 to 94 showed the forebrain containing ACC, in which the ACC were framed by dash lines. Sections from No. 104 to 130 showed the forebrain containing posterior cingulate cortex, in which the hippocampus were indicated by stars.

5.33 ± 0.12 mm, n = 18, 25, 32 slices in mouse, rat and tree shrew, respectively). We then estimated the volume of ACC as a sectorial cylinder (Figure 1(f) to (g)). Furthermore, we found that the volume of ACC in tree shrew was significantly larger than that of mouse and rat (mouse: $3.6 \pm 0.2\,mm^3$, rat: $42.7 \pm 3.9\,mm^3$, tree shrew: $58.3 \pm 6.6\,mm^3$, $p < 0.01$).

The cytoarchitecture of ACC

To describe the morphological properties of ACC in tree shrew, we carried out histochemical experiments in the rostral, medium and caudal regions of the ACC sections. As shown in the Nissl-stained slices (Figure 3), we found that ACC belongs to a granular cortex, containing molecular layer (I), external granular layer (II), well-developed external and internal pyramidal layers (III and V) and polymorphic layer (VI) but no internal granular layer (IV), which is in consistent with mouse and rat. The neuronal density of mouse ACC is greater than those of rat and tree shrew (mouse: $75.8 \pm 0.5\,mm^2$, n = 27 slices/4 animals; rat: $59.5 \pm 1.1\,mm^2$, n = 22 slices/3 animals, tree shrew: $51.3 \pm 1.4\,mm^2$, n = 25 slices/3 animals; $p < 0.05$). In addition, the molecular layer in tree shrew is thinner than that in mouse and rat (mouse: 0.35 ± 0.01 mm, n = 67 slices/4 animals; rat: 0.27 ± 0.01 mm, n = 35 slices/3 animals, tree shrew: 0.18 ± 0.01 mm, n = 46 slices/3 animals; $p < 0.05$).

NeuN is a neuronal-specific protein, distributed in the nucleus and cytoplasm of mature neurons. It was widely used as a marker for neuronal labeling.[23,24] In NeuN-immunostained slices, we found their distribution pattern was not different in mouse, rat and tree shrew, either in layer II/III or V/VI (Figure 4(a)). Similar to the results from Nissl staining, the density of NeuN-labeled neurons in tree shrew and rat was not different ($p > 0.05$) but less than that of mouse ($p < 0.01$) in both layers II/III (mouse: 1955.0 ± 32.6 neurons/mm^2, rat: 1575.0 ± 31.2 neurons/mm^2, tree shrew: 1410.5 ± 28.3 neurons/mm^2) and layers V/VI (mouse: 1550.8 ± 44.6 neurons/mm^2, rat: 1041.6 ± 25.6 neurons/mm^2, tree shrew: 1129.0 ± 32.5 neurons/mm^2) (n = 24 slices/4 animals in each group) (Figure 4(d)). We further analyzed the neuronal soma size and found the size in tree shrew and rat was similar ($p > 0.05$) but significantly larger than that of mouse ($p < 0.01$) in layer II/III (mouse: $100.0 \pm 3.5\%$, rat: $128.0 \pm 3.4\%$, tree shrew: $127.5 \pm 3.2\%$) and layer V/VI (mouse: $100.0 \pm 4.1\%$, rat: $118.1 \pm 7.0\%$, tree shrew: $131.4 \pm 9.3\%$) (n = 120 neurons/4 animals) (Figure 4(e)).

The neuronal morphology of ACC neurons

The Golgi staining is a well-established method for representing neuronal morphology. To evaluate the morphological characteristics of individual neuron, we used

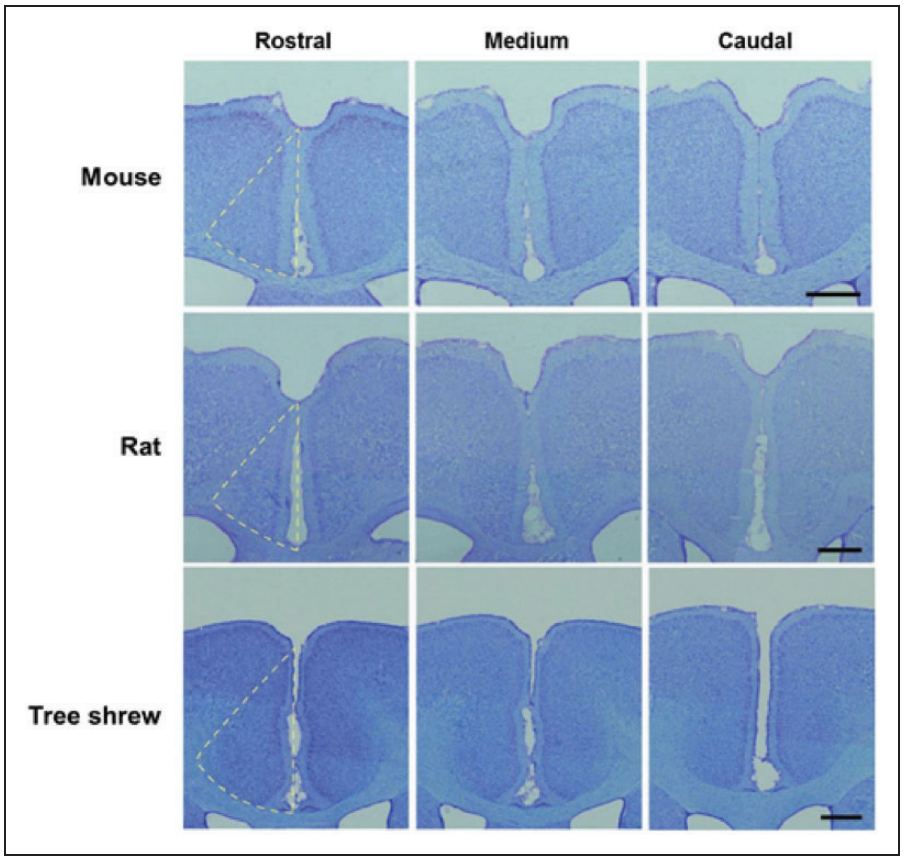

Figure 3. The rostral, medium and caudal part of ACC in tree shrew. Sample sections of Nissl staining showed the rostral, medium and caudal part of ACC in mouse, rat and tree shrew, respectively. The dash lines outline the areas of one side of ACC. Scale bar, 1 cm in mouse and 2 cm in rat and tree shrew.

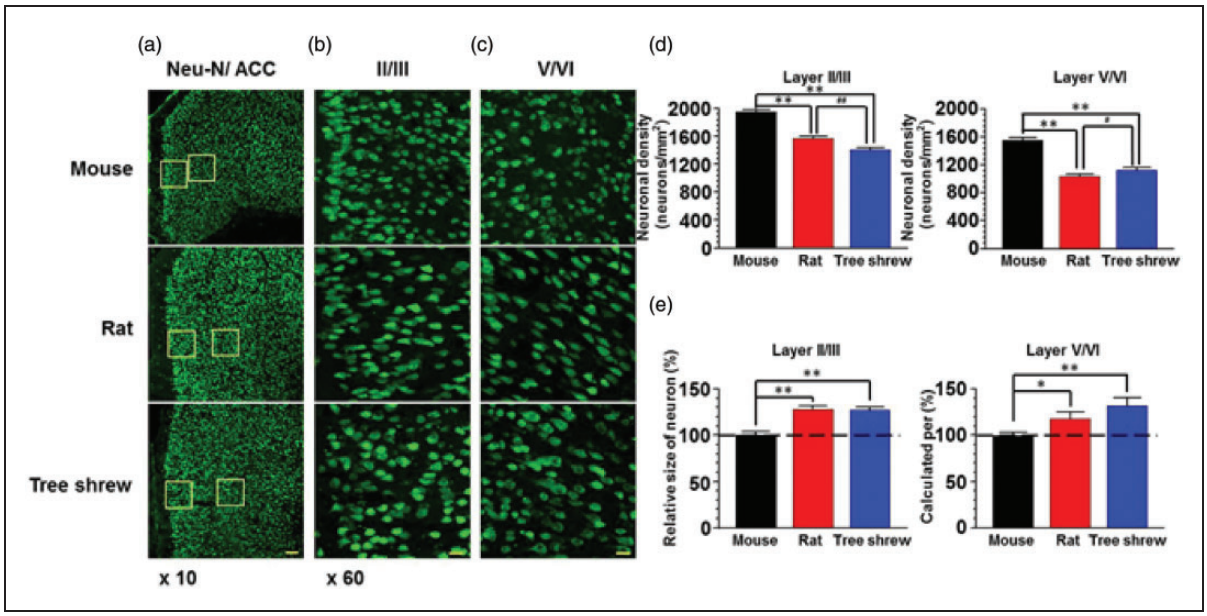

Figure 4. The neuronal distribution in the ACC of tree shrew. (a) Fluorescence images of NeuN-immunostained neurons in the ACC of mouse, rat and tree shrew. The frames in (a) were magnified to show the layers II/III (b) and V/VI (c) of the ACC. Scale bar, 100 μm in (a) and 20 μm in (b–c). (d) Summarized data showing that the neuronal density in layers II/III and V/VI of rat and tree shrew was less than that of mouse (n = 24 slices/4 animals in each group). $^{**}p < 0.01$ in comparison with mouse, $^{\#}p < 0.05$, $^{\#\#}p < 0.01$ in comparison with rat. (e) The neuronal size in layers II/III and V/VI of rat and tree shrew was larger than that of mouse. $^{*}p < 0.05$; $^{**}p < 0.01$.

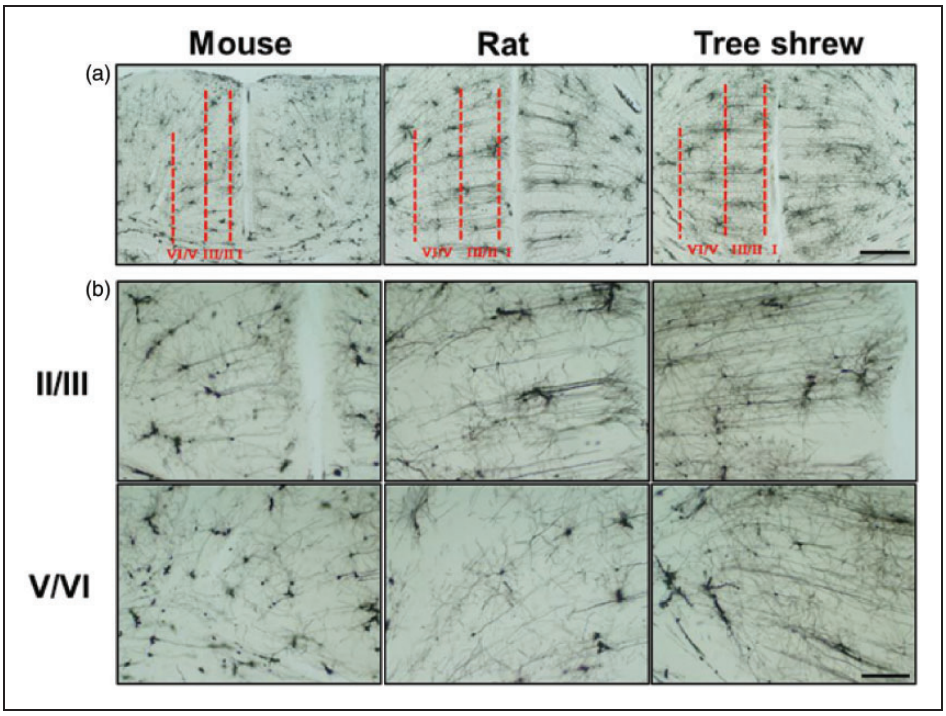

Figure 5. The distribution of Golgi-stained neuronal profiles in the ACC. (a) Lower magnification figures showing the Golgi impregnated neurons in the ACC of mouse, rat and tree shrew. Dashed lines delineate layer distribution of the ACC. (b) Higher magnification figures showing the neurons in layers II/III and V/VI.

Golgi impregnated sections in the ACC of mouse, rat and tree shrew (Figure 5(a), $n = 3$ in each group). The immunoreactive neurons were distributed from layer I to layer VI. Interneuron-like neurons could be observed in all layers, with smaller and round soma and short branches surrounding the soma. While pyramidal cell-like neurons were found in layer III, V and VI but not in layer I, with larger triangular soma, a long apical dendrite stretched toward shallow layers and basal dendrite with branches surrounding the soma (Figure 5(b)).

We then analyzed the apical and basal dendritic branches by introducing MOST method, in which micrometer-scale tomography of a centimeter-sized whole brain could be obtained.[21] Thus, the three-dimensional profiles of Golgi-stained ACC neurons at the neurite level could be reconstructed. The morphology and spatial locations of neuronal soma and branches could be clearly distinguished. We observed that the apical but not basal dendrites in the tree shrew and rat extended longer than that of the mouse (Figure 6(a)). To confirm whether the number of branches was different, the Sholl analysis method was then processed for analyzing randomly selected layer V neurons in mouse, rat and tree shrew (Figure 6(b)).[25] By quantifying the extent and complexity of neural processes, we found that the amount and distribution of dendritic branching in tree shrew were significantly different with rat and mouse. In tree shrew, the number of dendritic branches was larger than that of mouse and rat, at a distance from 60 to 260 μm away from the soma for basal dendrites and from 120 to 260 μm away from soma for apical dendrites (Figure 6(c)). In addition, the average number of basal dendritic branches (mouse: 126.8 ± 11.6, rat: 122.9 ± 10.2, tree shrew: 220.4 ± 18.5, $p < 0.01$) and apical dendritic branches (mouse: 75.5 ± 7.6, rat: 106.5 ± 10.5, tree shrew: 166.9 ± 12.7, $p < 0.01$) of tree shrew was also larger than that of mouse and rat ($n = 27$ neurons/3 animals in each group) (Figure 6(d)). Finally, although the apical dendrite of rat extended longer than that of mouse, the number of basal and apical dendritic branches were not different between rat and mouse ($p > 0.05$).

The spine morphology and density were also analyzed by assessing the apical dendritic spine of layer V neurons in the three types of animals. We found that the spine morphology was similar in mouse, rat and tree shrew, most of which were mushrooms like and with stubby heads (Figure 7(a)). However, the density of spines was progressively increased in mouse, rat and tree shrew ($p < 0.01$), and the average density of spines of tree shrew was also larger than that of mouse and rat (mouse: 7.0 ± 0.3, rat: 10.9 ± 0.8, tree shrew: 14.3 ± 0.7, $p < 0.01$) ($n = 27, 28, 27$ neurons/3 animals for mouse, rat and tree shrew, respectively) (Figure 7(b) to (c)).

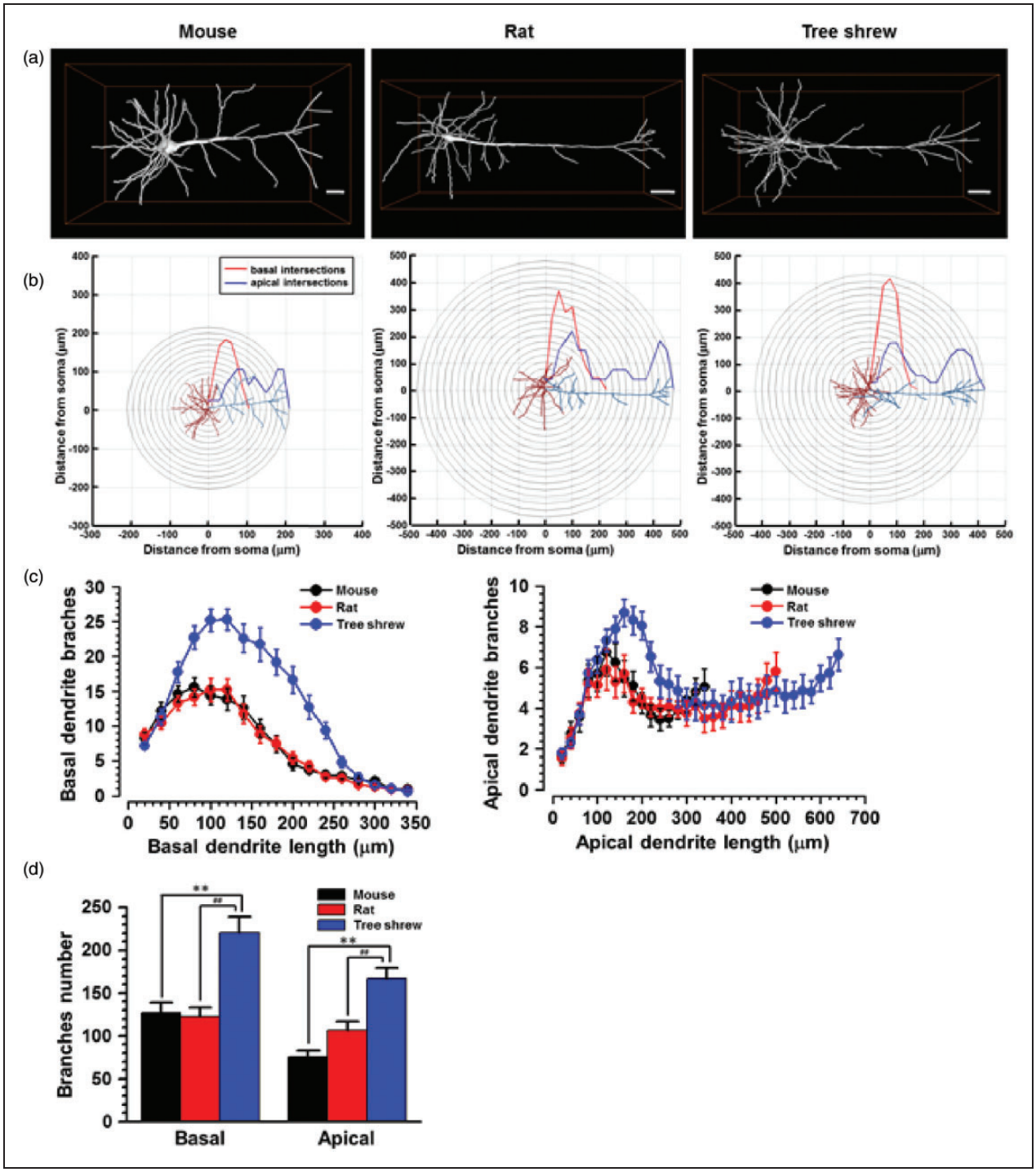

Figure 6. The basal and apical dendritic branches of the layer V pyramidal cell-like neurons in the ACC reconstructed by MOST. (a) Sample figures showing the reconstructed pyramidal cell-like neurons in layer V of ACC of mouse, rat and tree shrew. (b) Basal (red) and apical (blue) dendritic branches of a sample neuron under a concentric shell template for the Sholl analysis. Curves showed the average number of basal (red) and apical (blue) dendritic intersections per shell. (c) The number of basal and apical dendritic branches per 20 μm away from the soma. (d) The average number of basal and apical dendritic branches. $^{**}p < 0.01$ in comparison with mouse, $^{\#\#}p < 0.01$ in comparison with rat.

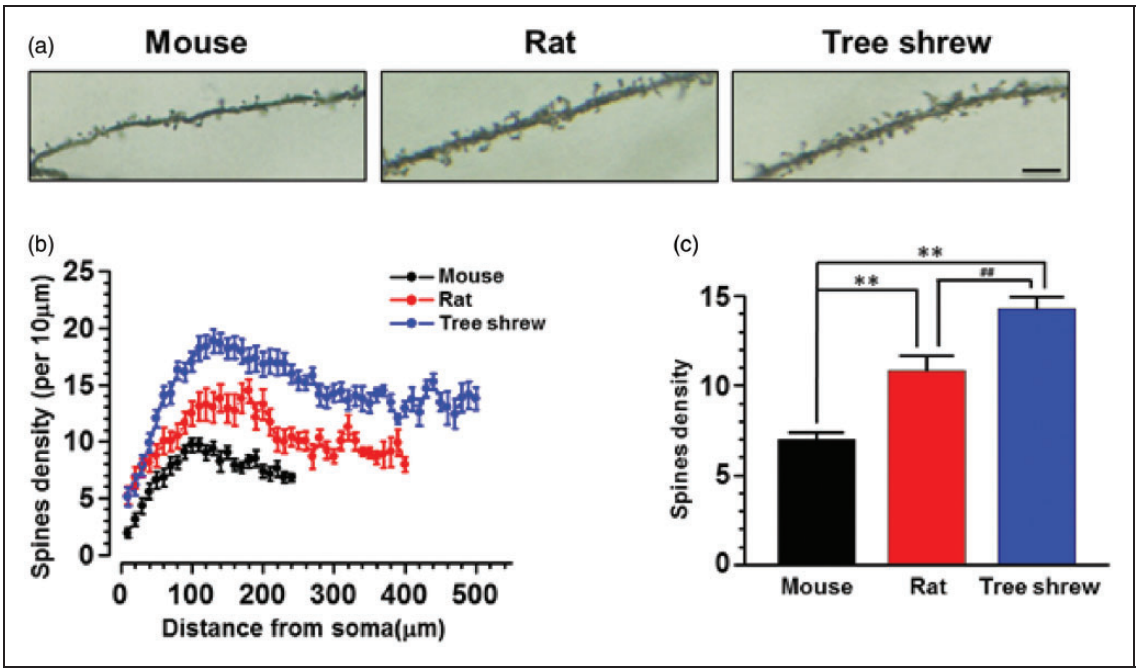

Figure 7. The density of spines in the apical dendrite of layer V pyramidal cell-like neurons in the ACC. (a) Representative figures showing spine distribution in the apical dendrites of ACC neurons from mouse, rat and tree shrew. (b) Pooled data showing the spine density per 10 μm along the apical dendrite (n = 27 neurons in mouse and tree shrew, n = 28 neurons in rat). (c) Averaged spine density in the apical dendrite. $^{**}p < 0.01$ in comparison with mouse, $^{\#\#}p < 0.01$ in comparison with rat.

Discussion

In the present study, we characterize the morphological properties of the ACC in tree shrew as compared with rodents (mouse and rat). We found that the proportions of brain and ACC in tree shrew were higher than those in mouse and rat. Furthermore, the ACC pyramidal cells are larger, with more abundant dendritic branches and spines in tree shrew. This finding is similar to previous reports in other tree shrew cortical areas.[7,19,20] Our studies suggest that ACC in tree shrew is more advanced than that of rodents (mouse and rat), indicating tree shrew could be considered as a useful primate-like animal model for studying the cellular mechanism for ACC-related physiological and pathological changes in human.

ACC is a key cortical region for pain and pleasure

Among several cortical regions, ACC is thought to be one of the key areas controlling human emotion including pain and pleasure. Previous human imaging studies have provided strong evidence that ACC is activated by unpleasant or pleasure stimuli, such as acute pain,[26–28] chronic pain[3] and anxiety,[29,30] as well as romantic love,[31,32] sex arouse[33–35] and attraction.[4] Cumulative studies at cellular and synaptic levels have shown that plasticity of excitatory transmission in the ACC play important roles in these emotion-related functions.[4,5,36–39] However, these results are mainly collected from the rodent models and less is available in primate models. We propose that the tree shrew provides a potential useful model for the convenient investigation of the neuronal intrinsic properties and synaptic plasticity in the primates.

Better developed pyramidal neuron in ACC of tree shrew

The morphological property of ACC in tree shrew has not yet been reported. In the present study, we found that the orientation, relative location, topography, laminar organization (layer I, II, III, V and VI) and general cytoarchitecture of ACC were similar among mouse, rat and tree shrew, in accordance with that reported in primates. The result suggests that the ACC belong to the conservatively developed brain areas. A significant difference among tree shrew and rodents is the more complex dendritic branching and increased spine density in the pyramidal cells of tree shrew, indicating these neurons will have more close synaptic connections with each other or with interneurons and they can contribute to the process of complicated information. It has been reported that the pyramidal cells in visual cortex of tree shrew have

more branches and the pattern of branches is similar to that of primates.[20]

Tree shrew is an animal model for the translation from rodents to human patients

Rodent animals such as mouse and rat have been widely used in biomedical research and contributed much to our understanding of mechanisms of disease including chronic pain.[1,2] Unfortunately, due to the fundamental biological difference in the species, some results from studies on rodent animals failed to be translated into human treatments. Furthermore, rodents also have significantly shorter lifespans and the effects of treatments on rats are therefore tested over a few weeks, whereas numerous chronic diseases last for several years, even decades, in humans, including chronic pain, post-herpetic neuralgia, diabetic neuropathy and Alzheimer disease.[40–42] Thus, key information related to the disease development and treatment effect will be lost from the rodents studies. For example, the amyloid accumulations and somatostatin degeneration are involved in impairments of cognitive functions during aging. An accumulation of amyloid β showed in the cerebral cortex neurons of aged macaque monkeys and tree shrews, but not in those of mouse and rat.[43] Similarly, somatostatin-immunoreactive senile plaque-like structures are found in the nucleus accumben of aged macaque monkey and tree shrew, but not in mouse and rat.[6] Therefore, additional animal models like tree shrew, which can live for more than 10 years, are clearly helpful for future translational drug discoveries.

In sum, we believe that the tree shrew is an ideal animal model for the study of synaptic mechanism in primates, not only for its closed genome with primates but also for its similar brain structure, cellular morphological and functional properties. The small body size, low cost of breeding, short reproductive cycle and long lifespan provide more reliability and convenience for the research works in both the cellular and behavioral level. In fact, the tree shrew has already been selected for the testing of drug efficacy and safety[44] and studies of the tree shrew will definitely provide more valuable information to reveal basic mechanisms of physiological and pathological brain changes in the future.

Acknowledgments

The authors thank Emily England for English editing.

Authors' contributions

Jing-Shan Lu performed the experiments, analyzed data and drafted the manuscript; Fang Yue and Xiaoqing Liu finished the Nissl and Golgi staining experiments. Min Zhuo and Tao Chen conceived and designed the research and finished the final version of the manuscript. All authors read and approved the final manuscript.

Declaration of Conflicting Interests

The author(s) declared no potential conflicts of interest with respect to the research, authorship, and/or publication of this article.

Funding

The author(s) disclosed receipt of the following financial support for the research, authorship, and/or publication of this article: This work was supported by grants from China Postdoctoral Science Foundation (2013M540740), NSFC (31371126 to TC) and grants from the EJLB-CIHR Michael Smith Chair in Neurosciences and Mental Health, Canada Research Chair, Canadian Institute for Health Research operating Grants (PJT-148648), NSERC Discovery Grant (RGPIN 402555) and the Azrieli Neurodevelopmental Research Program and Brain Canada (MZ).

References

1. Zhuo M. Cortical excitation and chronic pain. *Trends Neurosci* 2008; 31: 199–207.
2. Zhuo M. Neural mechanisms underlying anxiety-chronic pain interactions. *Trends Neurosci* 2016; 39: 136–145.
3. Bushnell MC, Ceko M and Low LA. Cognitive and emotional control of pain and its disruption in chronic pain. *Nat Rev Neurosci* 2013; 14: 502–511.
4. Wu LJ, Kim SS, Li XY, et al. Sexual attraction enhances glutamate transmission in mammalian anterior cingulate cortex. *Mol Brain* 2009; 2: 9.
5. Bliss TV, Collingridge GL, Kaang BK, et al. Synaptic plasticity in the anterior cingulate cortex in acute and chronic pain. *Nat Rev Neurosci* 2016; 17: 485–496.
6. Yamashita A, Fuchs E, Taira M, et al. Somatostatin-immunoreactive senile plaque-like structures in the frontal cortex and nucleus accumbens of aged tree shrews and Japanese macaques. *J Med Primatol* 2012; 41: 147–157.
7. Wong P and Kaas JH. Architectonic subdivisions of neocortex in the tree shrew (Tupaia belangeri). *Anat Rec (Hoboken)* 2009; 292: 994–1027.
8. Elston GN and Fujita I. Pyramidal cell development: postnatal spinogenesis, dendritic growth, axon growth, and electrophysiology. *Front Neuroanat* 2014; 8: 78.
9. Albon J, Farrant S, Akhtar S, et al. Connective tissue structure of the tree shrew optic nerve and associated ageing changes. *Invest Ophthalmol Vis Sci* 2007; 48: 2134–2144.
10. Drenhaus U, VonGunten A and Rager G. Classes of axons and their distribution in the optic nerve of the tree shrew (Tupaia belangeri). *Anat Rec* 1997; 249: 103–116.
11. Poveda A and Kretz R. c-Fos expression in the visual system of the tree shrew (Tupaia belangeri). *J Chem Neuroanat* 2009; 37: 214–228.
12. Bartolomucci A, de Biurrun G, Czeh B, et al. Selective enhancement of spatial learning under chronic psychosocial stress. *Eur J Neurosci* 2002; 15: 1863–1866.
13. Ohl F, Michaelis T, Vollmann-Honsdorf GK, et al. Effect of chronic psychosocial stress and long-term cortisol treatment on hippocampus-mediated memory and

hippocampal volume: a pilot-study in tree shrews. *Psychoneuroendocrinology* 2000; 25: 357–363.
14. Zambello E, Fuchs E, Abumaria N, et al. Chronic psychosocial stress alters NPY system: different effects in rat and tree shrew. *Prog Neuropsychopharmacol Biol Psychiatry* 2010; 34: 122–130.
15. Cao J, Yang EB, Su JJ, et al. The tree shrews: adjuncts and alternatives to primates as models for biomedical research. *J Med Primatol* 2003; 32: 123–130.
16. Fan Y, Huang ZY, Cao CC, et al. Genome of the Chinese tree shrew. *Nat Commun* 2013; 4: 1426.
17. Xu L, Chen SY, Nie WH, et al. Evaluating the phylogenetic position of Chinese tree shrew (Tupaia belangeri chinensis) based on complete mitochondrial genome: implication for using tree shrew as an alternative experimental animal to primates in biomedical research. *J Genet Genomics* 2012; 39: 131–137.
18. Keuker JIH, Rochford CDP, Witter MP, et al. A cytoarchitectonic study of the hippocampal formation of the tree shrew (Tupaia belangeri). *J Chem Neuroanat* 2003; 26: 1–15.
19. Sur M, Weller RE and Kaas JH. Representation of the body-surface in somatosensory area-I of tree shrews, Tupaia glis. *J Comp Neurol* 1980; 194: 71–95.
20. Elston GN, Elston A, Casagrande V, et al. Areal specialization of pyramidal cell structure in the visual cortex of the tree shrew: a new twist revealed in the evolution of cortical circuitry. *Exp Brain Res* 2005; 163: 13–20.
21. Li AA, Gong H, Zhang B, et al. Micro-optical sectioning tomography to obtain a high-resolution atlas of the mouse brain. *Science* 2010; 330: 1404–1408.
22. Cuntz H, Forstner F, Borst A, et al. One rule to grow them all: a general theory of neuronal branching and its practical application. *PLoS Comput Biol* 2010; 6: e1000877.
23. Gittins R and Harrison PJ. Neuronal density, size and shape in the human anterior cingulate cortex: a comparison of Nissl and NeuN staining. *Brain Res Bull* 2004; 63: 155–160.
24. Blaya MO, Bramlett HM, Naidoo J, et al. Neuroprotective efficacy of a proneurogenic compound after traumatic brain injury. *J Neurotrauma* 2014; 31: 476–486.
25. Shim SS, Hammonds MD and Mervis RF. Four weeks lithium treatment alters neuronal dendrites in the rat hippocampus. *Int J Neuropsychopharmacol* 2013; 16: 1373–1382.
26. Yoshino A, Okamoto Y, Onoda K, et al. Sadness enhances the experience of pain via neural activation in the anterior cingulate cortex and amygdala: an fMRI study. *Neuroimage* 2010; 50: 1194–1201.
27. Eisenberger NI, Lieberman MD and Williams KD. Does rejection hurt? An fMRI study of social exclusion. *Science* 2003; 302: 290–292.
28. Apkarian AV, Bushnell MC, Treede RD, et al. Human brain mechanisms of pain perception and regulation in health and disease. *Eur Jurnal Pain* 2005; 9: 463–484.
29. Wise RG, Lujan BJ, Schweinhardt P, et al. The anxiolytic effects of midazolam during anticipation to pain revealed using fMRI. *Magn Reson Imaging* 2007; 25: 801–810.
30. Osuch EA, Ketter TA, Kimbrell TA, et al. Regional cerebral metabolism associated with anxiety symptoms in affective disorder patients. *Biol Psychiatry* 2000; 48(10): 1020–1023.
31. Fisher HE, Aron A and Brown LL. Romantic love: a mammalian brain system for mate choice. *Philos Trans R Soc Lond B Biol Sci* 2006; 361: 2173–2186.
32. Bartels A and Zeki S. The neural basis of romantic love. *Neuroreport* 2000; 11: 3829–3834.
33. Arnow BA, Desmond JE, Banner LL, et al. Brain activation and sexual arousal in healthy, heterosexual males. *Brain* 2002; 125: 1014–1023.
34. Karama S, Lecours AR, Leroux J, et al. Areas of brain activation in males and females During viewing of erotic film excerpts. *Hum Brain Mapp* 2002; 16: 1–13.
35. Ferretti A, Caulo M, Del Gratta C, et al. Dynamics of male sexual arousal: distinct components of brain activation revealed by fMRI. *Neuroimage* 2005; 26: 1086–1096.
36. Wei F and Zhuo M. Potentiation of sensory responses in the anterior cingulate cortex following digit amputation in the anaesthetised rat. *J Physiol* 2001; 532: 823–833.
37. Yang JW, Shih HC and Shyu BC. Intracortical circuits in rat anterior cingulate cortex are activated by nociceptive inputs mediated by medial thalamus. *J Neurophysiol* 2006; 96(6): 3409–3422.
38. Koga K, Li XY, Chen T, et al. In vivo whole-cell patch-clamp recording of sensory synaptic responses of cingulate pyramidal neurons to noxious mechanical stimuli in adult mice. *Mol Pain* 2010; 6: 62.
39. Koga K, Descalzi G, Chen T, et al. Coexistence of two forms of LTP in ACC provides a synaptic mechanism for the interactions between anxiety and chronic pain. *Neuron* 2015; 85: 377–389.
40. Schreiber AK, Neufeld M, Jesus CHA, et al. Peripheral antinociceptive effect of anandamide and drugs that affect the endocannabinoid system on the formalin test in normal and streptozotocin-diabetic rats. *Neuropharmacology* 2012; 63: 1286–1297.
41. Hasnie FS, Breuer J, Parker S, et al. Further characterization of a rat model of varicella zoster virus-associated pain: relationship between mechanical hypersensitivity and anxiety-related behavior, and the influence of analgesic drugs. *Neuroscience* 2007; 144: 1495–1508.
42. du Sert NP and Rice ASC. Improving the translation of analgesic drugs to the clinic: animal models of neuropathic pain. *Br J Pharmacol* 2014; 171: 2951–2963.
43. Yamashita A, Fuchs E, Taira M, et al. Amyloid beta (Abeta) protein- and amyloid precursor protein (APP)-immunoreactive structures in the brains of aged tree shrews. *Curr Aging Sci* 2010; 3: 230–238.
44. Dixit R and Boelsterli UA. Healthy animals and animal models of human disease(s) in safety assessment of human pharmaceuticals, including therapeutic antibodies. *Drug Discov Today* 2007; 12: 336–342.